Diphenylpyrazoles as Replication Protein A Inhibitors
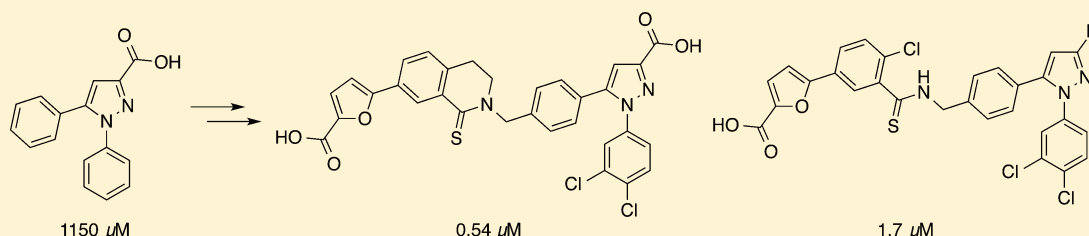
Alex G. Waterson,[‡,§] J. Phillip Kennedy,[†,||] James D. Patrone,[†] Nicholas F. Pelz,[†] Michael D. Feldkamp,[†] Andreas O. Frank,[†,⊥] Bhavatarini Vangamudi,[†,#] Elaine M. Souza-Fagundes,[†,○] Olivia W. Rossanese,[†] Walter J. Chazin,[†,§] and Stephen W. Fesik*[,†,‡,§]

[†]Department of Biochemistry, [‡]Department of Pharmacology, Vanderbilt University School of Medicine, and [§]Department of Chemistry, Vanderbilt University, Nashville, Tennessee 37232, United States

S *Supporting Information*

ABSTRACT: Replication Protein A is the primary eukaryotic ssDNA binding protein that has a central role in initiating the cellular response to DNA damage. RPA recruits multiple proteins to sites of DNA damage via the N-terminal domain of the 70 kDa subunit (RPA70N). Here we describe the optimization of a diphenylpyrazole carboxylic acid series of inhibitors of these RPA−protein interactions. We evaluated substituents on the aromatic rings as well as the type and geometry of the linkers used to combine fragments, ultimately leading to submicromolar inhibitors of RPA70N protein−protein interactions.

KEYWORDS: *Replication protein A, fragment-based discovery, medicinal chemistry*

Replication Protein A (RPA), the eukaryotic ssDNA binding protein, is a widely used scaffold for DNA transactions that functions by protecting and organizing ssDNA, as well as recruiting other proteins of the DNA processing machinery.[1,2] RPA is a heterotrimer; the 70-kDa subunit contains an OB-fold at its N-terminus, RPA70N, that serves as a protein recruitment module.[1−3] In particular, this domain plays a crucial role in recruiting DNA damage response and repair proteins to sites of DNA damage, via a conserved motif that interacts with a basic cleft at the surface of RPA70N.[4−6]

Given the critical role of the RPA70N interactions with target proteins in initiating DNA damage response, inhibition of these interactions has the potential to suppress damage response pathways and may represent a promising approach for enhancing the effect of DNA damaging agents. A selective inhibitor of the RPA70N−protein interactions that does not abrogate ssDNA binding or important scaffolding activities of the entire protein would provide a powerful tool for focused exploration of the role of RPA in checkpoint signaling and enable studies to confirm the therapeutic potential of RPA70N inhibition. In addition, such a compound would represent a potential starting point for new cancer drugs. Indeed, a recent report describes a small molecule that binds to RPA70N and demonstrates activity in a xenograft tumor model.[7]

Toward the discovery of new inhibitors, we have reported the use of a fragment-based screen to identify small molecules that bind to the basic cleft of RPA70N, the elaboration of these fragments to produce two triazole series (**1** and **2**), and

preliminary linking efforts to obtain molecules (e.g., **3**) that span the entire cleft (Figure 1).[8,9] Here, we describe the optimization of the linked compounds, including the details of the structure−activity relationships (SAR) for binding to RPA70N and the physicochemical properties of selected compounds.

The synthetic route used to produce linked compounds such as **3**[8] was adapted to explore the SAR of the diphenylpyrazoles and linked compounds described herein. The basic route involves a cyclodehydration reaction to generate functionalized diphenylpyrazoles that are elaborated in various ways to construct the inhibitor compounds. Full details of the compound syntheses are reported in the Supporting Information.

We explored the SAR of the 1,5-diphenyl pyrazoles via chemical synthesis and targeted purchasing (Table 1). The initial analogues were evaluated for binding to RPA70N using HSQC NMR-based titrations. Of note, the carboxylic acid was critical for binding, as all analogues devoid of this acid, or with ester or amide derivatives, displayed sharply reduced binding affinity to the protein (not shown).

We quickly established a preference for 3- and 4-position substituents on this ring (compare **4a** versus **4c,d**). The most robust trend evident in this initial group was a very strong preference for halogens in the 3- and 4-positions of the 1-
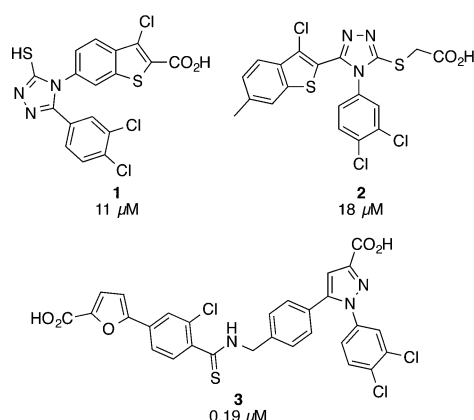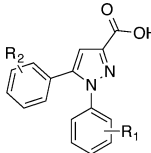
Figure 1. Previously reported RPA70N inhibitors.[8,9] Values represent binding affinities determined in an FPA assay.
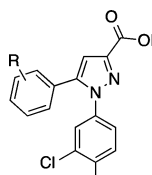
Table 1. Pyrazole SAR in Site-1

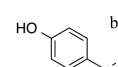| Cpd	R_1	R_2	NMR K_d (μM)[a]	K_d (μM)[b]	% inh[c]	LE[d]
4a	H	-H	1150			0.21
4b	4-OMe	-H	895	>500	18	0.19
4c	3-Me	-H	580	>500		0.22
4d	4-Cl	4-Cl	260	>500	24	0.23
4e	2,4-diCl	4-Cl	410	>500	29	0.21
4f	3,4-diCl	4-Cl	54	67 ± 9		0.25
4g	3-Me	4-OMe		>500	20	N/A
4h	4-Me	4-OMe		>500	15	N/A
4i	3-Br	4-OMe		140 ± 2.8		0.23
4j	4-Br	4-OMe		>500	24	N/A
4k	3-Cl	4-OMe		>500	35	N/A
4l	4-Cl	4-OMe		>500	19	N/A
4m	3,4-diCl	4-OMe		79 ± 1.4		0.24
4n	cyclohexyl[e]	4-OMe		>500	9	N/A

[a]K_d values determined from 6 point NMR titrations. [b]Average K_d values (n = 2) calculated using Cheng−Prusoff equation from IC$_{50}$ values measured in FPA competition assay. [c]Amount of displacement of labeled probe at the highest compound concentration used, 500 μM. [d]LE = ligand efficiency. Values calculated using LE = 1.4pK_d/HAC, using FPA data if available and NMR data if the FPA data did not give a K_d value. [e]Represents replacement of the entire phenyl ring.

phenyl ring (e.g., **4f**). Indeed, we found a distinct binding affinity advantage for a 3,4-dichlorophenyl substitution, mirroring the preference found in a prior series of RPA70N binding compounds and in a potent stapled helix peptide inhibitor of RPA70N.[9,10] It is likely that the halogen substituents lead to additional hydrophobic interactions and a possible halogen bond in the lipophilic cavity near Ser55 in RPA70N (Site-1) in which the *N*-phenyl ring of the pyrazole compounds bind.[8]

Compound **4f** displayed sufficient NMR-derived binding affinity to also be evaluated in an FPA competition assay,[11] which produced a comparable binding affinity of 67 μM. This assay was used exclusively to profile later analogues. To identify additional substituents that might effectively fill Site-1, we
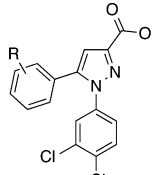
Table 2. Pyrazole 5-Position SAR

Cpd	R	Kd (μM)[a]	LE[c]
4f	4-Cl	67 ± 9	0.25
5a	H	123 ± 4.2	0.25
5b	3-Me	90 ± 1.4	0.25
5c	4-Me	72 ± 4.9	0.25
5d	3-CO$_2$H	129 ± 17	0.22
5e	4-CO$_2$H	59 ± 3.5	0.24
5f	4-CN	310 ± 21	0.20
5g	4-CH$_2$NH$_2$	>500	N/A
5h	4-NH$_2$	227 ± 27	0.22
5i	4-OH	104 ± 15	0.24
5j	4-(2-furanyl)[b]	>500	N/A
5k	[b]	>500	N/A

[a]Average K_d values (n = 2) calculated using Cheng-Prusoff equation from IC$_{50}$ values measured in FPA competition assay. [b]Entire ring system replaces the phenyl. [c]LE = ligand efficiency. Values calculated using LE = 1.4pK_d/HAC, using the FPA data.
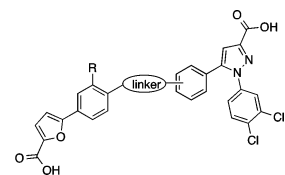
Table 3. Extension of the Diphenylpyrazoles

Cpd	R	K_d (μM)[a]	LE[b]
4f	4-Cl	67 ± 9	0.25
6a	4-CONHCH$_2$(phenyl)	83 ± 18	0.18
6b	4-CONHCH$_2$(4-methoxyphenyl)	45 ± 11	0.18
6c	4-CH$_2$NHCO(phenyl)	90 ± 15	0.18
6d	4-CH$_2$NHCO(4-methoxyphenyl)	72 ± 7.8	0.17
6e	4-CH$_2$NHCO(4-bromophenyl)	35 ± 2.1	0.19
6f	4-CSNHCH$_2$(phenyl)	18 ± 6.4	0.21
6g	4-CSNHCH$_2$(4-methoxyphenyl)	23 ± 4.2	0.19
6h	4-CH$_2$NHCS(4-bromophenyl)	15 ± 1.4	0.20
6i	4-CH$_2$NHSO$_2$(phenyl)	70 ± 9.2	0.17
6j	4-CH$_2$NHSO$_2$(4-trifluoromethoxyphenyl)	56 ± 2.8	0.16

[a]Average K_d values (n = 2) calculated using Cheng−Prusoff equation from IC$_{50}$ values measured in FPA. [b]LE = ligand efficiency. Values calculated using LE = 1.4pK_d/HAC, using the FPA data.

initiated a more thorough investigation of the 1-phenyl ring SAR, systematically exploring lipophilic and halogen substitutions at the 3- and 4- positions, using a 4-methoxyphenyl ring at the pyrazole 1-position as a standard substitution. Unfortu-

Table 4. Fragment Linking and Optimization

Cpd	R	Linker	Linker position	K_d (μM)[a]	LE[b]
7a	H		para	57±1.4	0.15
7b	H		para	8.2±2.6	0.17
7c	H		meta	22±4.2	0.16
7d		-[c]	para	2.5±0.1	0.20
7e	H		para	1.5±0.3	0.20
7f	H		para	0.55±0.1	0.22
7g	Cl		para	9.4±3.8	0.17
7h	Cl		para	0.48±0.1	0.22
7i[8]	Cl		para	2.9±0.8	0.18
3[8]	Cl		para	0.19±0.03	0.23
7j	-		para	0.54±0.2	0.21

[a]Average K_d values (n = 2) calculated using Cheng−Prusoff equation from IC_{50} values measured in FPA. [b]LE = ligand efficiency. Values calculated using LE = $1.4pK_d$/HAC, using the FPA data. [c]The linker is attached to the meta position of the furan phenyl ring and the para position of the pyrazole phenyl ring.

nately, most of these analogues displayed a loss of binding affinity 10-fold or greater compared with **4f**, with only the 3-Br analogue **4i** producing a full concentration−response curve. Some rank ordering of the compounds was determined by examining the maximal displacement of the FPA probe at the highest compound concentration. From this, it was generally evident that 3-position substitutions were favored over 4-position substitutions and that a bromine was favored over chlorine or methyl at the 3-position. Larger substitutions in either the 3- or 4-position, for example, the use of bicyclic ring systems and larger alkyl groups such as isopropyl, were completely ineffectual (data not shown). However, as observed with **4f**, combining the 3- and 4-chloro substitutions produces a large gain in binding affinity (**4m**). Finally, we established an advantage for a phenyl substituent on the 1-position of the pyrazole (compare **4n** versus **4a**).

Holding the 3,4-dichlorophenyl substitution pattern constant, we initiated an investigation of 5-phenyl ring

modifications. In general, a relatively wide range of substitutions was tolerated with minimal changes in binding affinity or ligand efficiency (LE) (Table 2). We observed a slight preference for 4-position substitutions over 3-position analogues (**5b** vs **5c**, **5d** vs **5e**). A 4-cyano substituent was 4-fold less potent than the methyl analogue (**5b** v. **5f**) and the corresponding amine-containing **5g** was completely inactive. While some polar groups were tolerated in this region (e.g., **5d**, **5e**, **5h**, and **5i**), heterocyclic ring systems were generally disfavored (e.g., **5j**). In addition, a methylene could not be introduced between the pyrazole and the phenyl ring without a substantial loss of binding affinity (e.g., **5k**).

Many SAR trends in this series can be rationalized by the cocrystal structures of the molecules bound to the basic cleft of RPA70N. As previously described,[8] 1,5-diarylpyrazoles bind with good affinity to Site-1 and are located above Ser55 in the protein. The 3,4-dichloro substitution more effectively fills the Site-1 pocket compared with other substitution patterns. Interestingly, the 4-position chloride is located 3.5−3.8 Å away from the side chain oxygen of Ser 55, at bond angles of 150−160°, indicating a possible halogen bond interaction. In addition, the 5-position phenyl ring is located such that substitutions at the 3- and 4-positions are aimed directly down the basic cleft. Thus, it is reasonable to expect that a range of modifications would be tolerated on this ring. The hydrophobic nature of the central portion of the cleft may also explain the poor binding affinity of the basic amine-containing **5g**.

Because the 5-phenyl ring is ideally positioned in the cleft of RPA70N to tolerate larger functionality, we elected to employ a fragment growing strategy to seek affinity improvements. Using the carboxylic acid of **5e** and the amine of **5g** as synthetic handles, we synthesized an exploratory series of substituted amides, thioamides, and sulfonamides with phenyl moieties predicted to extend down the cleft of RPA70N (Table 3). Most of the amide and sulfonamide analogues failed to demonstrate substantial improvement over **4f** or **5e**. In general, the best analogues within this group (**6e−h**) employ highly lipophilic thioamide-containing substitutions and display binding affinities 2−3-fold better than **4f**. As these substitutions did not add significant affinity to the molecules to offset large increases in molecular weight, the corresponding ligand efficiencies are lower. However, it should be noted that the thioamides had generally higher ligand efficiencies than their amide counterparts, indicating the likelihood of a specific interaction. Interestingly, several attempts to replace the appended phenyl rings with heterocycles produced compounds with extremely weak binding to the protein (data not shown), reinforcing the preference for lipophilic substitutions in this region of the protein.

Fragment linking to generate high affinity inhibitors is considered difficult to achieve, due to the specific geometrical constraints that must be precisely matched to successfully link two molecules that bind to adjacent sites in a protein. However, several successful examples demonstrate the power of this approach.[12] RPA70N appeared ideally suited for this strategy, as a single fragment screen identified multiple series of fragments that bind to two different, nearby sites in the protein.

An ether linker should provide flexibility and allow a linked compound to achieve a binding pose similar to the original fragments. However, connecting the optimized diphenylpyrazole and a furan-based fragment with either a two atom link[8] or a longer, PEG-inspired 4 atom link (data not shown) proved less successful than anticipated. We virtually docked prospective
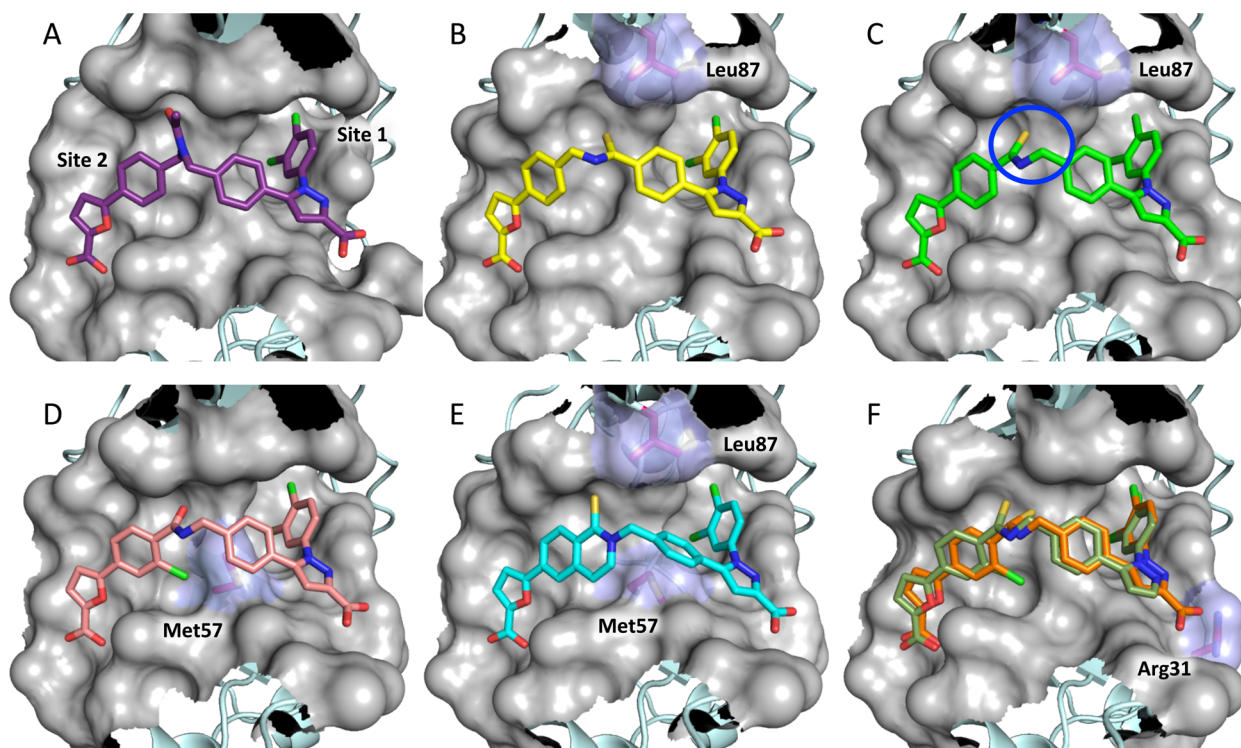
Figure 2. X-ray cocrystal structures of compounds in complex with RPA70N: (A) compound **7b** (PDB 4R4Q), (B) compound **7e** (4R4O), (C) compound **7f** (4R4T), (D) compound **7i** (4R4C), (E) compound **7j** (4R4I), and (F) compound **11** (green, 4LWC) overlaid with **3** (orange).
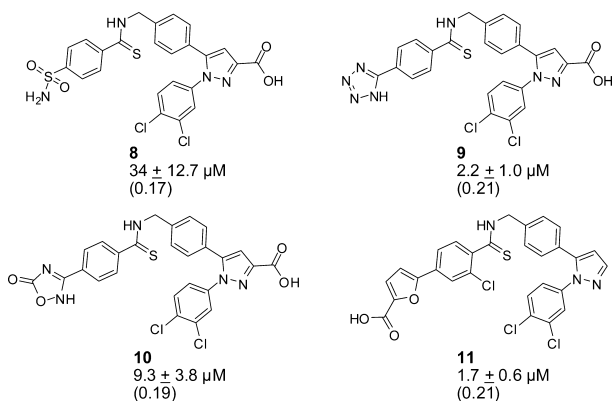

8
34 ± 12.7 μM
(0.17)

9
2.2 ± 1.0 μM
(0.21)

10
9.3 ± 3.8 μM
(0.19)

11
1.7 ± 0.6 μM
(0.21)

Figure 3. Linked compounds with acid replacements. Average K_d values ($n = 2$) calculated using Cheng–Prusoff equation from IC_{50} values measured in FPA. Ligand efficiency (LE) values in parentheses.

molecules into RPA70N using the Induced Fit Docking Protocol available from Schroedinger.[13] This suggested exploration of three atom linkers. Thus, we used the amine of **5g** as a synthetic handle (Table 4). The initial compound, **7a**, reinforced the lack of tolerance for a charged atom in this region of the protein. Acetylating this amine produced a 10-fold gain in binding affinity (**7b**). However, the binding mode of the compound in complex with RPA70N reveals a linker conformation that is kinked to accommodate the requirements of the original fragment molecules in Site-1 and Site-2 (Figure 2A).

Further molecular modeling also suggested that an sp² hybridized carbon in the linker would improve the binding geometry. This idea was explored in the context of both meta- and para-linked compounds, with a carbonyl or thiocarbonyl attached to the 5-phenyl ring of the pyrazole. In accordance

with the computational predictions, linkers with an sp² center were generally superior to those with saturated linkers. We found a distinct preference for a more lipophilic thioamide substitution over the amide (**7c** vs **7e**, **7g** vs **7h**). The thioamide appears to occupy a small hydrophobic space under Leu87 (Figure 2B), potentially explaining the enhanced binding affinity granted by this substitution. Placing the linker on the 3-position of the furan phenyl ring offered no significant advantage over the 4-position (**7d** vs **7e**). In addition, placement of the thioamide carbonyl on the furan phenyl ring was found to be superior to placement on the 5-phenyl pyrazole (**7f** vs **7e**). The structure of **7f** in complex with RPA70N reveals that the sulfur is able to access the Leu87 pocket with less contortion of the linker portion of the molecule (blue circle, Figure 2C), leading to a compound with submicromolar binding affinity to RPA70N.

Introduction of a 3-position chloride (inspired by the fragment SAR)[8] on the phenylfuran produced affinity gains over the des-chloro variants (e.g., **7h** vs **7e**, **3** vs **7f**), probably due to the occupation of space in the binding site above Met57 (Figure 2D). The application of all of these strategies produced compounds with the highest binding affinity to RPA70N and with ligand efficiencies similar to the original pyrazole-containing compounds (**3**).[8] A cyclic thioamide linker (**7j**) also places nonpolar atoms under Leu87, occupies the space above Met57 (Figure 2E), and binds with submicromolar affinity.

We explored removal or replacement of one or both of the two carboxylic acids from the high affinity linked compounds to guard against possible issues with poor cellular permeability. Indeed, we assessed the permeability of compound **3** in the Caco-2 cell line and found that it possesses poor intrinsic permeability of $<0.21 \times 10^{-6}$ cm/s and is subject to significant pgp-mediated efflux (efflux ratio > 32). Applying the optimal

143

dx.doi.org/10.1021/ml5003629 | ACS Med. Chem. Lett. 2015, 6, 140−145

thioamide positioning, we explored isosteres of the 2-furan carboxylic acid designed to maintain the key binding interactions with Arg31 (8−10, Figure 3). The best of these compounds (9) displays low micromolar binding affinity. We also explored the removal of the pyrazole carboxylic acid. Compound 11, devoid of this carboxylic acid, has a 1.7 μM binding affinity to RPA70N in our FPA assay and an intrinsic permeability of 14.5×10^{-6} cm/s, with no pgp efflux noted. The X-ray cocrystal structure of this molecule, overlaid with the previously reported structure of 7j (Figure 2F), demonstrates that the lack of interaction with Arg31 leads to a slight relaxation of the molecule in the pocket and a slight shift toward Site-2. This shift, and the missing interaction with Arg31, may explain the 10-fold loss in binding affinity compared with 3.

Interactions mediated by the RPA70N domain of RPA are essential for recruiting a number of key proteins to initiate DNA damage response and repair (e.g., ATRIP, MRE11, RAD9). Each of these interactions is mediated by the binding of RPA70N to an amphiphilic helix from the target protein. The amphiphilic nature of the RPA70N binding site seems to produce strict requirements for a tightly binding compound, as evidenced by our optimization efforts. A significant amount of hydrophobic contact area must be engaged, and the binding must be anchored by interaction with charged residues at the outer edges of the cleft.

We have generated molecules with submicromolar binding affinity to this cleft using fragment linking and subsequent optimization. The requirements to successfully bind to the basic cleft of RPA70N result in small molecules with relatively poor pharmaceutical properties. Careful molecular design to remove one of the negatively charged groups, yet maintain the other important contributors to binding affinity, has produced a compound with enhanced permeability. However, this trade-off results in loss of binding affinity to the protein, pointing toward opportunities for future optimization. The molecules described here represent a useful starting point for obtaining potent and cell permeable RPA inhibitors that could be used as tools to validate that inhibition of the RPA70N−protein interactions is a therapeutically relevant avenue for suppression of the DNA damage response as an adjuvant cancer treatment.

ASSOCIATED CONTENT

Ⓢ Supporting Information

Synthetic procedures, compound characterization, and assay protocols. This material is available free of charge via the Internet at http://pubs.acs.org.

Accession Codes

The atomic coordinates and structure factors for the X-ray crystal structures of RPA70N in complex with compounds 7b (4R4Q), 7e (4R4O), 7f (4R4T), 7i (4R4C), 7j (4R4I), and 11 (4LWC) have been deposited in the Protein Data Bank RCSB PDB.

AUTHOR INFORMATION

Corresponding Author

*Tel: 615-322-6303. E-mail: stephen.fesik@vanderbilt.edu.

Present Addresses

∥(J.P.K.) Revance Therapeutics, Newark, California 94560, United States.

⊥(AO.F.) Novartis Institutes for BioMedical Research (NIBR), Global Discovery Chemistry, Emeryville, California 94608, United States.

#(B.V.) UT MD Anderson Cancer Center, Houston, Texas 77054, United States.

○(E.M.S.-F.) Federal University of Minas Gerais, Belo Horizonte, Brazil.

ACKNOWLEDGMENTS

We would like to thank Dr. David Cortez for his intellectual contributions in the conception of this project.

REFERENCES

(1) Wold, M. S. Replication protein A: A heterotrimeric, single-stranded DNA-binding protein required for eukaryotic DNA metabolism. Annu. Rev. Biochem. 1997, 66, 61−92.

(2) Wold, M. S.; Kelly, T. Purification and characterization of replication protein-a, a cellular protein required for invitro replication of simian virus-40 DNA. Proc. Natl. Acad. Sci. U.S.A. 1988, 85, 2523−2527.

(3) Xu, X.; Vaithiyalingam, S.; Glick, G. G.; Mordes, D. A.; Chazin, W. J.; Cortez, D. The basic cleft of RPA70N binds multiple checkpoint proteins, including RAD9, to regulate ATR signaling. Mol. Cell. Biol. 2008, 28, 7345−7353.

(4) Fanning, E.; Klimovich, V.; Nager, A. R. A dynamic model for replication protein A (RPA) function in DNA processing pathways. Nucleic Acids Res. 2006, 34, 4126−4137.

(5) Cortez, D.; Guntuku, S.; Qin, J.; Elledge, S. J. ATR and ATRIP: Partners in checkpoint signaling. Science 2001, 294, 1713−1716.

(6) Cimprich, K. A.; Cortez, D. ATR: an essential regulator of genome integrity. Nat. Rev. Mol. Cell Biol. 2008, 9, 616−627.

(7) Glanzer, J. G.; Liu, S.; Wang, L.; Mosel, A.; Peng, A.; Oakley, G. G. Cancer Res. 2014, 74, 5165−5172.

(8) Frank, A. O.; Feldkamp, M. D.; Kennedy, J. P.; Waterson, A. G.; Pelz, N. F.; Patrone, J. D.; Vangamudi, B.; Camper, D. V.; Rossanese, O. W.; Chazin, W. J.; Fesik, S. W. Discovery of a potent inhibitor of replication protein a protein-protein interactions using a fragment-linking approach. J. Med. Chem. 2013, 56, 9242−9250.

(9) Patrone, J. D.; Kennedy, J. P.; Frank, A. O.; Feldkamp, M. D.; Vangamudi, B.; Pelz, N. F.; Rossanese, O. W.; Waterson, A. G.; Chazin, W. J.; Fesik, S. W. Discovery of protein-protein interaction inhibitors of replication protein A. ACS Med. Chem. Lett. 2013, 4, 601−605.

(10) Frank, A. O.; Vangamudi, B.; Feldkamp, M. D.; Souza-Fagundes, E. M.; Luzwick, J. W.; Cortez, D.; Olejniczak, E. T.; Waterson, A. G.; Rossanese, O. W.; Chazin, W. J.; Fesik, S. W. Discovery of a potent stapled helix peptide that binds to the 70N domain of replication protein A. *J. Med. Chem.* **2014**, *57*, 2455−2461.

(11) Souza-Fagundes, E. M.; Frank, A. O.; Feldkamp, M. D.; Dorset, D. C.; Chazin, W. J.; Rossanese, O. W.; Olejniczak, E. T.; Fesik, S. W. A high-throughput fluorescence polarization anisotropy assay for the 70N domain of replication protein A. *Anal. Biochem.* **2012**, *421*, 742−749.

(12) Ichihara, O.; Barker, J.; Law, R. J.; Whittaker, M. Compound design by fragment-linking. *Mol. Inform.* **2011**, *30*, 298−306.

(13) *Schrödinger Suite 2009 Induced Fit Docking Protocol; Glide version 5.5; Prime version 2.1*; Schrödinger, LLC: New York, 2009.

145

dx.doi.org/10.1021/ml5003629 | *ACS Med. Chem. Lett.* 2015, 6, 140−145